Astronomy
&
Astrophysics

An EUV Bright Point as seen by SUMER, CDS, MDI and EIT on-board SoHO

M. S. Madjarska[1], J. G. Doyle[1], L. Teriaca[2], and D. Banerjee[3]

[1] Armagh Observatory, College Hill, Armagh BT61 9DG, N. Ireland
[2] Osservatorio Astrofisico di Arcetri, Largo E. Fermi 5, 50125 Firenze, Italy
[3] Centre for Plasma Astrophysics, Katholieke Universiteit Leuven, Celestijnenlaan 200B, 3001 Leuven, Belgium

Abstract. This paper presents the formation, evolution and decay of a coronal bright point via a spectroscopic analysis of its transition region counterpart and the evolution of the underlying magnetic bipole during 3 days of almost continuous observations. The data were obtained with various instruments on-board SoHO, including the SUMER spectrograph in the transition region line S VI 933.40 Å, CDS in the He I 584.33, O V 629.73 and Mg IX 368.06 Å lines, plus MDI and EIT. The existence of the coronal feature is strongly correlated with the evolution of the underlying bipolar region. The lifetime of the bright point from the moment when it was first visible in the EIT images until its complete disappearance was ~18 hrs. Furthermore, the bright point only became visible at coronal temperatures when the two converging opposite magnetic polarities were ~7000 km apart. As far as the temporal coverage of the data permits, we found that the bright point disappeared at coronal temperatures after a full cancellation of one of the magnetic polarities. The spectroscopic analysis reveals the presence of small-scale (~6″) transient brightenings within the bright point with a periodicity of ~6 min. The Doppler shift in the bright point was found to be in the range of −10 to 10 km s^{-1} although it is dominated by a red-shifted emission which is associated with regions characterized by stronger "quiet" Sun photospheric magnetic flux. Small-scale brightenings within the bright point show velocity variations in the range 3–6 km s^{-1}. In general the bright point has a radiance ~4 times higher than that of the network. No relation was found between the bright point and the UV explosive event phenomena.

Key words. Sun: corona – Sun: transition region – Sun: activity – Sun: UV radiation

1. Introduction

Coronal X-ray/EUV bright points (hereafter BPs) are among the coronal phenomena claimed to play an important role in the coronal heating problem. They were first identified in the X-rays in 1969 by Vaiana et al. (1970) and later analysed and described in detail during the Skylab mission (for reviews see Golub 1980; Webb 1986; Habbal 1992). BPs are small (30″–40″ size) coronal features of enhanced emission with a 5″–10″ bright core. They were associated with small bipolar magnetic features, except for newly emerging or old and decaying BPs where only one of the polarities is visible (Golub et al. 1977). They were found in the "quiet" Sun regions and coronal holes, at the network boundaries where the "quiet" Sun magnetic field is mainly concentrated (Habbal et al. 1990). Sheeley & Golub (1979) obtained a unique sequence of high resolution Naval Research Laboratory (NRL) *Skylab* spectroheliograms with a spatial resolution of ~2″. They showed that the coronal BPs pattern consists of 2 or 3 miniature loops (2 500 km in diameter and ~12 000 km long) evolving on a time scale of ~6 min. Observations by Habbal et al. (1990) confirmed this

result showing that simultaneously measured peaks of emission in six different lines (emitted from the chromosphere to the corona) were not always co-spatial, implying that the BPs consist of a complex of small-scale loops at different temperatures. The average lifetime of a BP is ~20 hrs (Zhang et al. 2001) as observed in EUV lines and 8 hrs as determined by *Skylab* X-ray observations (Golub et al. 1974). Zhang et al. (2001) suggested that the temperature of BPs is generally below 2×10^6 K, which explains their smaller size and shorter lifetime in X-rays.

BPs were also observed in the transition region and chromosphere, where some of them appeared at a low contrast with a brightness similar to the brightness of the network elements (Habbal & Withbroe 1981; Habbal et al. 1990; Habbal 1992). Using the High Resolution Telescope and Spectrograph (HRTS), Moses et al. (1994) performed a spectroscopic study aimed at investigating the correspondence of small-scale structures from different temperature regimes in the solar atmosphere and in particular the relationship between X-ray BPs (XBPs) and UV transition region explosive events. They found that the features in C IV 1548 Å corresponding to XBPs were in general bright, larger scale (~10″) regions of complex velocity fields of the order of 40 km s^{-1} which, according to the authors, is typical for the brighter C IV network elements.

They also concluded that the transition region explosive events do not correspond directly to XBPs.

Webb et al. (1993) found that XBPs are associated with the cancellation of network, intranetwork or ephemeral region magnetic fields. These authors concluded that nearly all XBPs (88%) are associated with converging magnetic features of opposite polarity, irrespective of their origin. They observed that some XBPs are present even before the onset of cancellation although this result may very much depend on the instrumental resolution. XBPs are more than twice as likely to be associated with decaying or canceling magnetic features than with emerging or growing ones (Webb et al. 1993). Priest et al. (1994) presented a two-dimensional model (a converging flux model) of BPs based on the interaction of two sources of opposite magnetic polarity with the same strength, situated in an overlying uniform magnetic field. Later the model was further developed by Parnell et al. (1994b) for interaction of two magnetic sources with an opposite sign, but different strengths which agrees with the main XBPs and canceling magnetic features observations. A three-dimensional model for reconnection was also developed by Parnell et al. (1994a). Langcope (1998) developed a minimum current coronal model (three-dimensional) using measurable quantities and a few free parameters to make quantative predictions of morphology and power loss in a single XBP.

The Solar and Heliospheric Observatory (SoHO) provided the first opportunity for simultaneous observations of the solar atmosphere from the photosphere to the solar corona. Observations obtained by four of the instruments on-board SoHO, the Extreme-ultraviolet Imaging Telescope (EIT), the Solar Ultraviolet Measurements of Emitted Radiation (SUMER) spectrograph, the Coronal Diagnostics Spectrometer (CDS) and the Michelson Doppler Imager (MDI) enable studies of coronal structures together with their counterpart in the transition region, chromosphere and underlying longitudinal photospheric magnetic field. The higher temporal, spatial and spectral resolution of the present generation instruments enables us to study in this paper the formation, evolution and decay of a BP observed in EIT narrow-band images centered around the Fe XII 195 Å coronal line (1.6 10^6 K) together with the evolution of the underlying longitudinal magnetic field (MDI) during 3 days of almost continuous observations. SUMER observations were performed in the same region in the transition region S VI 933 Å and Ly 6 930 Å lines. The high resolution spectroscopic observations permitted us to determine the plasma flows within the BP through the Doppler shifts of one of the observed lines. The association of coronal BPs with transient phenomena such as explosive events and blinkers is also briefly discussed. In Sect. 2 we present the observational data while Sect. 3 presents the data analysis and results. The discussion and conclusions are given in Sect. 4.

2. Observational material

2.1. SUMER

The observations obtained with the SUMER spectrograph (for details see Wilhelm et al. 1995, 1997; Lemaire et al. 1997)
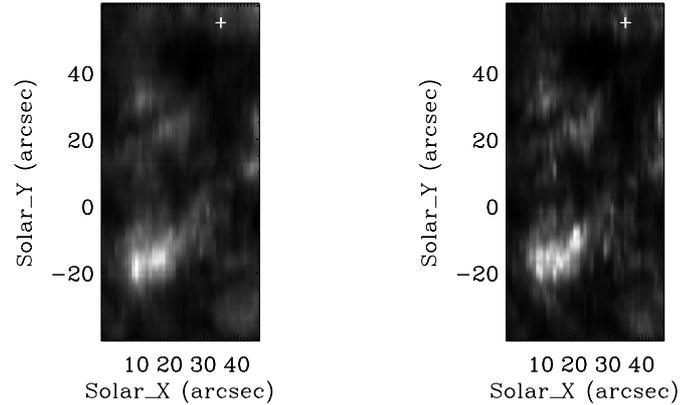

Fig. 1. SUMER radiance images in the Ly 6 930 Å (left) and S VI 933 Å (right) lines. The bright feature visible around solar_$Y = -20''$ was associated with a coronal bright point. The location of the explosive event (whose corresponding line profile is shown in Fig. 11) is marked by a cross in both images (top righthand corner).

represent high cadence temporal series in the transition region S VI 933.40 Å (200 000 K) and chromospheric/low transition region Ly 6 930.748 Å (20 000 K) lines. The dataset was obtained on 1996 October 17 and 18 in the "quiet" Sun at heliographic coordinates $X = 0''$ and $Y = 0''$. A $1'' \times 120''$ slit was used. The observations started on October 17 at 19:23 UT and finished on October 18 at 00:23 UT. The dataset consists of a full spectrum over the spectral range 907–954 Å obtained prior to each temporal series. The full spectra were obtained exposing a band of 120 spatial × 1024 spectral pixels from the central part of detector B for 200 s. The wavelength calibration for SUMER, which has no calibration source on-board, is usually done using chromospheric lines of neutral atoms. In the present study the full spectrum covers a few unblended O I lines such as O I 929.52 Å and O I 936.63 Å which were used as wavelength standards during the calibration. Since the reference lines are in general rather weak, we used profiles averaged along the slit to determine the centroids of these lines from a Gaussian fit. Both the Ly 6 and S VI lines were registered on the KBr part of the detector.

The temporal sequence consists of two spectral windows (120 spatial × 50 spectral pixels) centered on Ly 6 930.748 Å and S VI 933.40 Å, obtained with a 10 s exposure time. No compensation for the solar rotation was applied and therefore for a solar rotation at these heliographic coordinates of about $10''$/h, the $1''$ slit covered a region of $\sim 47''$.

The reduction of SUMER raw data involves local gain correction, flat-field subtraction and a correction for geometrical distortion. The signal to noise level was determined by the photon statistics.

In the present study we used only the S VI line at 933.40 Å. This line is blended in the red wing by He II Balmer 12 at 933.44 Å (Curdt et al. 1997, 2001). The blend effect accounts for about 10% (W. Curdt, private communication) of the feature at 933 Å. As will become evident later in the paper, this does not influence our results.
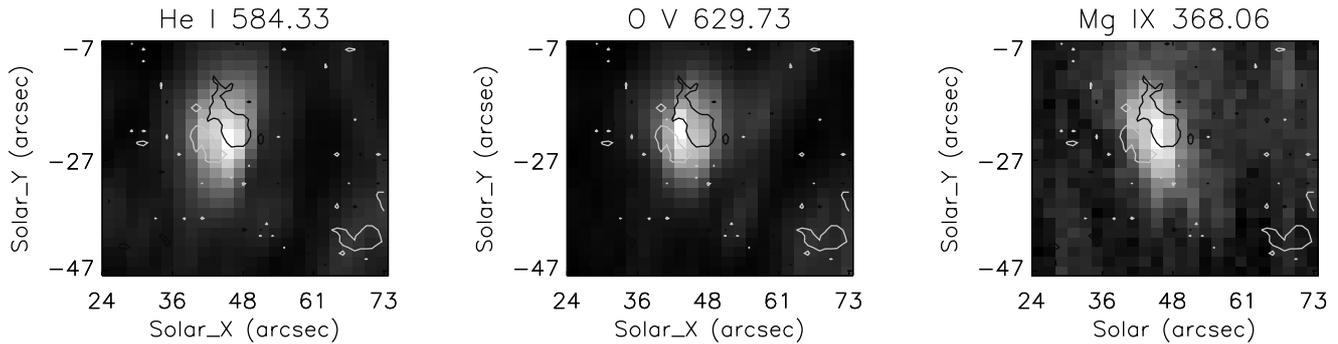
Fig. 2. A section of the CDS raster in the SUMER field-of-view obtained from 02:25 to 03:34 UT on October 18, (i.e. ~1 h 30 min after the last SUMER spectrum was registered) in the He ɪ, O v and Mg ɪx lines. A contour map of the longitudinal photospheric magnetic field registered by MDI is over-plotted. The white contours correspond to +25 G and the black ones to −25 G.
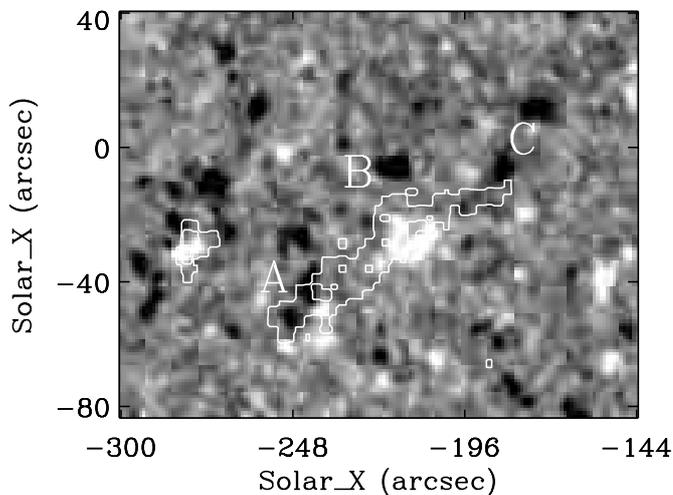

Fig. 3. MDI magnetogram scaled from −25 to +25 G obtained at 01:00 UT on October 17, with the over-plotted contour map of an EIT high resolution image obtained at 01:25 UT on October 17.

2.2. MDI

MDI (Scherrer et al. 1995) observations were performed on 1996 October 16, 17 and 18 during a coordinated observing program with EIT. MDI high resolution photospheric longitudinal magnetograms (0$\farcs$6 pixel^{-1}) were obtained with a 60 s exposure time and a field-of-view of 500×1024 pixels between 1996 October 17 15:21 UT and October 18 07:00 UT. A few full disk images with a field-of-view of 1024×1024 pixels (2″ pixel^{-1}) obtained on 1996 October 16 and 17 were also used.

2.3. EIT

The EIT (Delaboudinière et al. 1995) observations analysed in this study were obtained in Fe xɪɪ 195 Å (1.6×10^6 K) on 1996 October 16, 17 and 18. EIT was operating at two different regimes, 2×2 binned full-disk images with a resolution of 5$\farcs$24 and full-resolution (2$\farcs$62) part-disk images. The latter had a field of view of 512×512 pixels and were obtained from 01:25 UT to 22:25 UT on October 17 every 30 min. After

14:55 UT there was a gap of 3 hrs after which only three images were taken.

The data were obtained with a 60 s exposure time and were degridded, flat-fielded and dark-curve subtracted. Bright pixels due to cosmic rays or instrumental defects were selected visually and removed by replacing them with the mean of the first neighbour pixels.

2.4. CDS

The CDS (Harrison et al. 1995) data represent synoptic observations obtained in He ɪ 584.33 Å (~32 000 K), O v 629.73 Å (250 000 K) and Mg ɪx 368.06 Å (10^6 K) on October 18, 1996 from 02:25 UT to 03:34 UT. A raster $244'' \times 240''$ centered at solar_X = −2″ and solar_Y = −3″, was registered using a $2'' \times 240''$ slit with a 15 s exposure. The angular pixel size was 1$\farcs$68 in the solar_Y direction and of about 4″ in the solar_X direction. The standard CDS procedures were applied to correct for missing pixels, CCD readout bias, cosmic rays and flat field effects.

3. Data analysis and results

Due to the ~10″ hour^{-1} solar rotation, the SUMER $1'' \times 120''$ slit moved over a new solar region after 390 s. As a rough approximation we can adopt that ~39 spectra (each spectrum was obtained with 10 s exposure time) were taken over the same solar region. In Fig. 1 we show the reproduced raster of the $47'' \times 100''$ region of the solar disk obtained after 5 hrs of sit-and-stare observations. Besides the typical network pattern, the raster reveals a ~20″ × 20″ bright structure visible in both the S vɪ (200 000 K) and Ly 6 (~20 000 K) lines. The feature had a radiance of ~4 times higher than that of the network. It is impossible to identify any particular fine structure within the observed event, most likely due to the large resulting exposure time (390 s) of the raster. The same phenomenon, but with a smaller size, was also visible on the later (obtained between 02:25 and 03:34 UT on October 18) CDS rasters in He ɪ, O v and Mg ɪx (Fig. 2). In order to determine the nature of this phenomenon we analysed all EIT and MDI data available in the time period of 1 day before and after the SUMER and CDS observations were taken.

EIT coronal, SUMER and CDS transition region and magnetic field observations were coaligned as described below. First a co-alignment of EIT and MDI images with a large field-of-view (300″×300″ MDI high-resolution field of view) was made using as a reference photospheric magnetic field concentrations of different scales and their corresponding brightenings in the solar corona (Schrijver et al. 1997; Handy & Schrijver 2001). The next step was to co-align the SUMER and CDS (CDS observed in a rastering mode which makes it easier to compare the network pattern) with the MDI observations again using the network as a corresponding feature. We found a SUMER offset of ~9 arcsec in solar_Y and 5 arcsec in solar_X directions with respect to MDI and EIT.

The alignment revealed that the SUMER brightening is the transition region counterpart of a coronal bright point as identified in the EIT Fe xɪɪ images and the CDS Mg ɪx raster. The magnetic field pattern (MDI) showed that the BP was formed at a network junction and was associated with a small bipolar region (see Figs. 3 and 4).

3.1. Magnetic bipole and coronal brightening evolution

The formation of the BP followed a complicated scenario involving the formation and decay of a few coronal loops in the observed region. After inspecting all images as seen from different instruments, we could formulate the following sequences of events. The loop system was formed from a diffuse haze visible in Fe xɪɪ 195 Å at around 03:00 UT on October 16. Figure 5 presents a sequence of images of a selected 157″ × 124″ region from the full-disk binned and high-resolution part-disk EIT images. The sequence traces the formation and the disintegration of a complex loop system followed by a bright point formation, evolution and decay.

First at 09:00 UT on 16th a small loop was formed connecting the opposite polarities of a very small magnetic bipole which in Fig. 3 corresponds to the bipole B. Around 19:03 UT on the same day a bigger loop was formed connecting the predominant negative polarity of the bipole A (which had also a small loop structure) and the positive polarity of the bipole B (Fig. 3). Later on at 22:38 UT the coronal loop extended further north connecting the positive polarity of the bipole B with the negative polarity C (Fig. 3). To summarize, the extended double loop was shaped by two loops which connected two negative polarities situated on both sides (south-east (A) and north-west (C)) of the positive polarity of bipole B. In A, B and C small-scale loop structures were also present.

It has already been mentioned that the BP was found at a network junction. A MDI movie[1] shows that the junction was formed and continuously compressed by 4 or 5 evolving convective cells during the whole observing period. Small magnetic fragments were continuously driven by the plasma motions from the center of the cells towards their boundaries. After reaching the boundaries some of the magnetic features were canceling (if they were of opposite polarity) or were merging with one of the bipole polarities.

Despite the absence of high temporal and spatial resolution MDI observations between 01:25 UT and 15:21 UT on 17th, the few full disk MDI observations (at 08:03, 09:39, 11:15, 12:51 and 14:27 UT) together with the EIT images helped us to reconstruct the evolution of the underlying longitudinal magnetic field for this time period. The analysis of the EIT and MDI data revealed that the middle positive polarity of bipole B (Fig. 3) had moved towards the negative polarity C, which caused the creation of a small loop structure visible as a bright point (in C) around 11:25 on 17th in Fig. 5. Around 06:00 UT on October 17, the small loop system B-C faded and only a tiny loop remained visible. At 07:03 UT on 17th, one can see that the loop connecting A and B bipoles also started to fade (Fig. 5) and disappeared completely at around 12:00 UT. In fact, the continuous displacement of the middle positive polarity of bipole B towards C caused the two loops associated with these bipoles to fade away. At 13:55 UT two separate bright points were visible on the place marked as A and C in Fig. 3. At the time of the BP formation only one full-disk (2″ spatial resolution) MDI image was available (at 11:15 UT while the BP appears on the EIT images at 11:25). At that time the distance between the two polarities was ~7000 km.

The lifetime of the BP from the moment when it was first visible on the EIT images until its complete disappearance was ~18 hrs. An important observational fact is that the BP existed until the complete cancellation of one of the polarities (the moving one). MDI data showed that the cancellation finished at 05:26 UT on October 18. The EIT image on October 18 at 05:00 UT displayed the BP almost as a single EIT pixel of enhanced emission. At 07:00 UT (there were no Fe xɪɪ 195 images between 05:00 and 07:00 UT), the BP is no longer visible in the Fe xɪɪ images.

3.2. Magnetic flux and coronal emission

The evolution of the analysed magnetic bipole showed a total magnetic flux disappearance due to photospheric cancellation. Figure 6 shows that the total unsigned magnetic flux decrease is correlated with the BP radiance flux decrease registered in Fe xɪɪ/EIT. In this study the total unsigned magnetic flux profile ($\Phi = \int |B_l| dS$) was obtained by integrating the absolute longitudinal magnetic field strength $|B_l|$, over a rectangular array which includes the bipole region. The background was derived from an array showing no magnetic flux concentration and then subtracted. Such a correlation was already found by Preś & Phillips (1999), Handy & Schrijver (2001) and Zhang et al. (2001) using X-ray, EUV and MDI joint observations. Fisher et al. (1998) using a combined dataset of 333 vector magnetograms of active regions and their corresponding time averages of SXT full-frame images derived the relation between X-ray luminosity (L_X) and the global magnetic variables such as the total unsigned magnetic flux Φ, the longitudinal and transverse magnetic field strength B_l^2 and B_t^2, respectively and the longitudinal current density J_l. They found that the X-ray luminosity is highly correlated with all the global magnetic variables, but it is best correlated with the total unsigned magnetic flux. Unfortunately, the low number of datapoints in our intensity data does not allow us for such a detailed study.

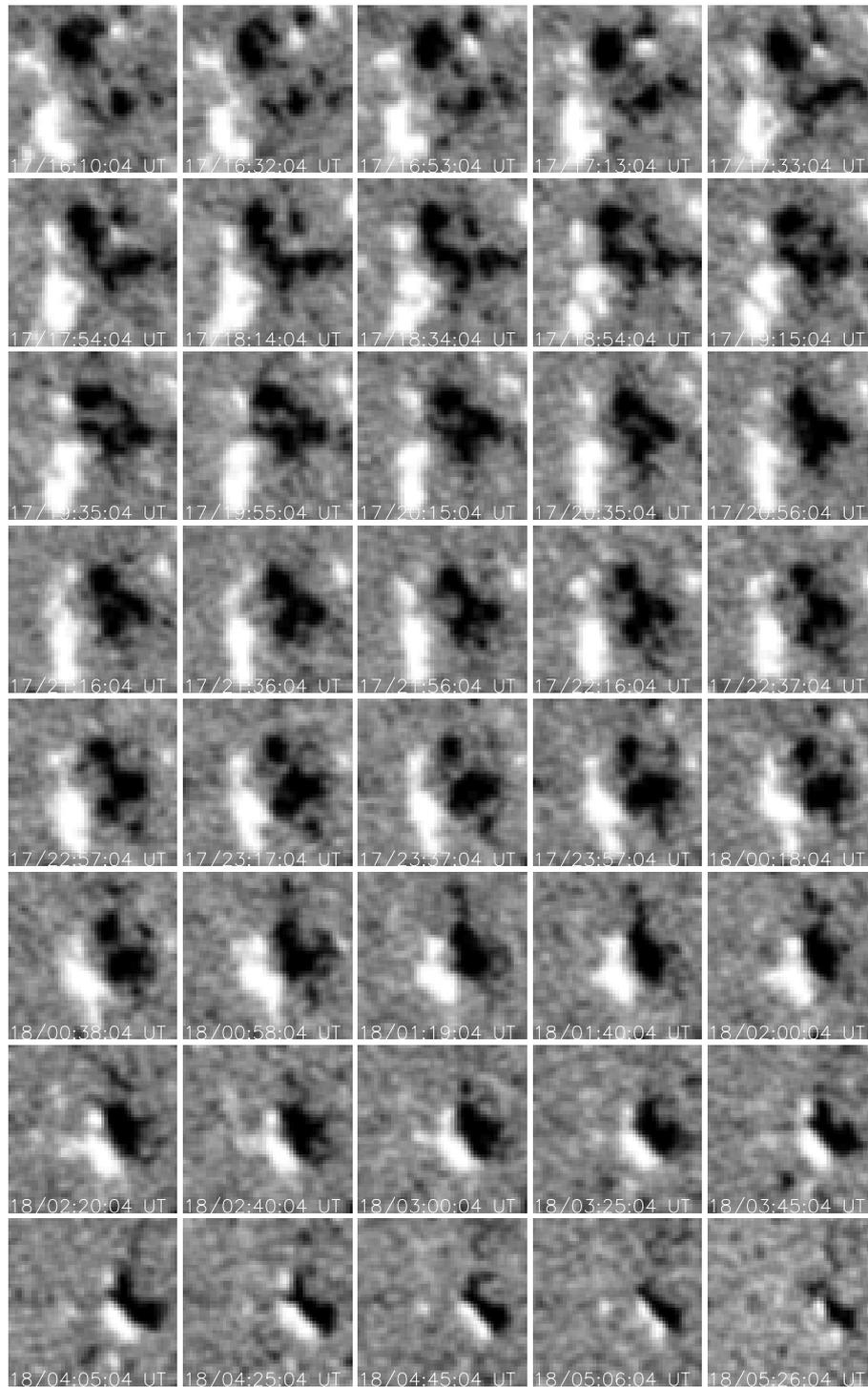
[1] http://star.arm.ac.uk/~madj/movie_mdi2.html

Fig. 4. The magnetic field temporal evolution of a bipolar region associated with the coronal bright point. The images have a 30″ × 30″ field-of-view, and were averaged over five frames with the scaling from −25 to +25 G. These frames cover the time period from 16:10 UT on October 17 to 05:26 UT on October 18.

Nevertheless, the good correlation between the total unsigned magnetic flux and the BP radiance flux is clearly seen (Fig. 6).

Handy & Schrijver (2001) also found that only a magnetic flux above a threshold of 3×10^{18} Mx was associated with a noticeable brightening in the EIT Fe xii corona. Therefore, emerging bipoles would appear as a brightening on SXT/Yohkoh images for only a small percentage of bipoles and/or with a shorter lifetime than in EUV as was found by Zhang et al. (2001). A simple explanation could be that the appearance at a certain temperature depends strongly on the magnetic energy released and, therefore, on the bipole magnetic field strength.
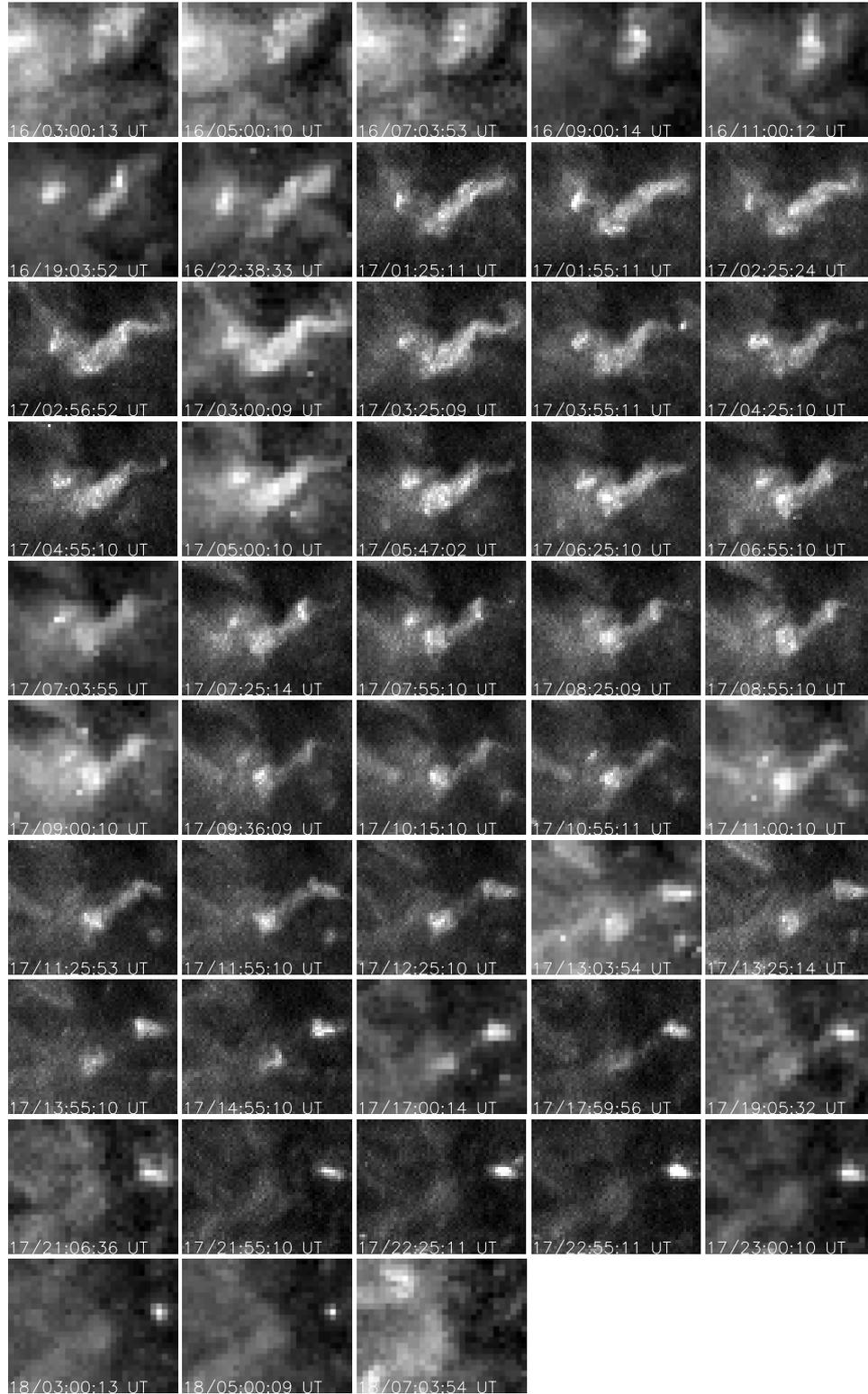
Fig. 5. Combined temporal sequence of binned 2×2 (5''24) full-disk and high-resolution (2''62) part-disk EIT Fe XII 195 Å images with a 157'' × 124'' field-of-view. The images were obtained from October 16 at 03:00 UT until October 18 at 07:00 UT.

3.3. BP spectroscopic analysis

Priest et al. (1994) presented a converging flux model of BPs based on the interaction of two sources of opposite magnetic polarity with the same strength, situated in an overlying uniform magnetic field. In their paper the authors raised many questions asking for more observational evidence on the observational properties of coronal bright points. Most of these questions, however, still remain unanswered because of the absence of a spectroscopic analysis of high spectral, temporal and spatial resolution observations of BPs. In our study we were
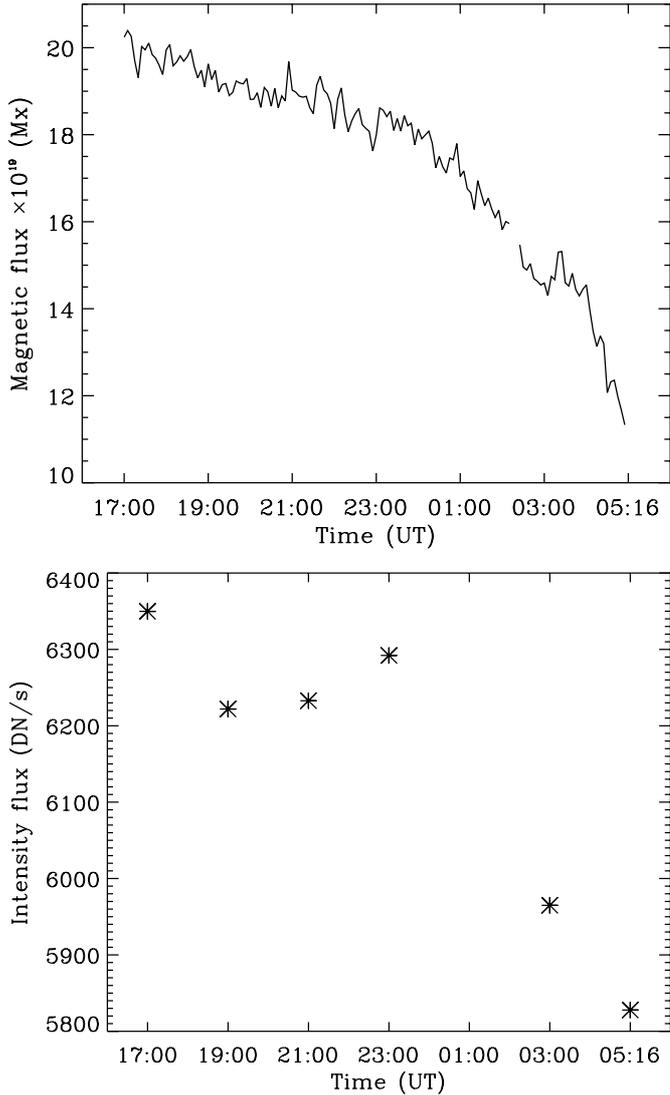
Fig. 7. *Left panel:* S VI radiance image with over-plotted magnetic field contours (white +25 G, black −25 G). *Right panel:* S VI radiance image with over-plotted velocity contours (white +3 km s⁻¹, black −3 km s⁻¹).

Fig. 8. *Left panel:* S VI Doppler shift image with over-plotted magnetic field contours (white +25 G, black −25 G). *Right panel:* EIT Fe XII 195 image with over-plotted magnetic field contours (white +25 G, black −25 G).

Fig. 6. *Upper panel:* integrated unsigned magnetic flux of the BP region as a function of time (14 hrs: from 17 October at 17:00 UT until 18 October at 05:00 UT). The missing values correspond to bad data. *Bottom panel:* integrated radiance flux (as recorded in Fe XII/EIT) of the BP region as a function of time. Only the full disk images were used because they cover the longest observing period.

fortunate that the SUMER spectrograph was pointed at a region which, at the same time, was observed by the EIT and MDI instruments. The 20″×20″ bright feature (see Fig. 1) was scanned by the SUMER slit in approximately 2 hours.

The SUMER observations were performed in two lines, Ly 6 930.748 Å, (20 000 K) and S VI 933.40 Å (200 000 K). The Ly 6 line is blended by O I 930.26 Å, He II 930.32 Å and O I 930.89 Å. These blends made it impossible to estimate the Doppler shift using this line. The line-of-sight velocity behaviour of the transition region counterpart of the BP was studied using the S VI line. The fitting of simulated line profiles show that a 10% blend of the He II Balmer 12 933.44 Å to the S VI line add only between 1 and 2 km s⁻¹ to the derived S VI Doppler shifts. Now we focus on the BP and the surrounding region. The left panel of Fig. 7 presents the S VI radiance image with an over-plotted contour map of the photospheric
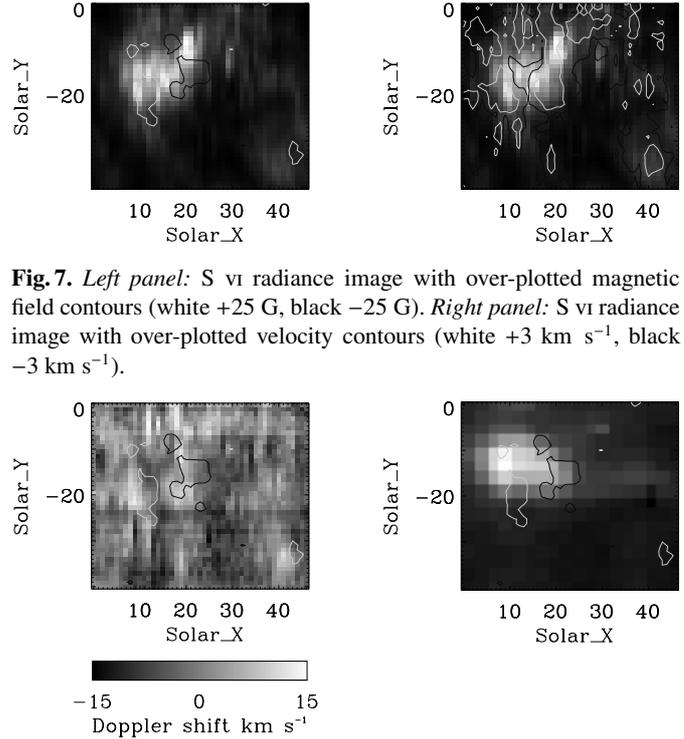
longitudinal magnetic field registered by MDI. The white contours correspond to a magnetic field of +25 G and the black −25 G. This image demonstrates the relation between the bipole structure and the corresponding transition region BP. The BP was scanned by SUMER in ∼2 hours and the over-plotted magnetic field contour map is taken close to the middle of this period.

The right panel of Fig. 7 is a compilation of a S VI radiance raster and over-plotted Doppler shift contours. The Doppler shift contour map clearly shows the pattern of the typical network red-shift. The BP is dominated by a red-shifted emission which is associated mainly with the regions characterized by stronger "quiet" Sun magnetic fields. This is best visible on the left panel of Fig. 8 where the Doppler shift image scaled from −15 to +15 km s⁻¹ is over-plotted with the −25 G (black) and +25 G (white) longitudinal magnetic field contours. The region between the two polarities shows a blue-shift pattern.

In order to study the temporal and spatial variation of the radiance and the Doppler shift, we bin over 5 consecutive spectra (with a resulting time resolution of ∼50 s), thereby also improving our signal to noise ratio. A "stretched" raster, in which each position corresponds to a 50 s exposure time, is shown in Fig. 9. In general the BP has a radiance ∼4 times higher than that of the network. The image in Fig. 9 revealed that the BP consists of small-scale, short-lived brightenings of ∼6″ solar_Y size (only the solar_Y size can be determined with the present observations) and ∼6 min duration. As was mentioned before, the SUMER slit covers a new region of the Sun after ∼390 s due to the solar rotation. Therefore, any
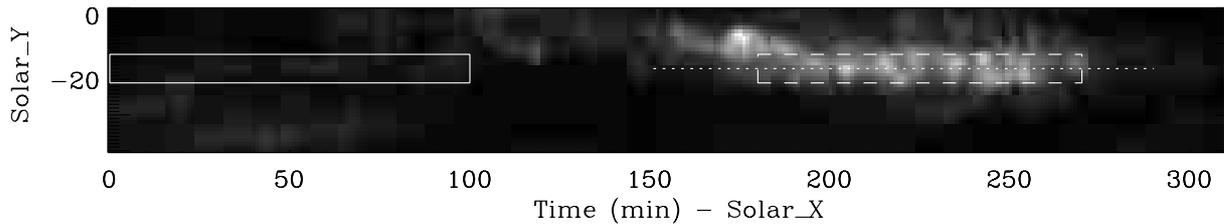
Fig. 9. The S VI radiance image with the dotted line showing the position at which the radiance and velocity profiles presented in Fig. 10 were obtained. The areas indicated with a solid and dashed lines represent the region which has been used to derive the line profile in the network and bright point, respectively.

variations occurring during a period of 400–500 s (which corresponds to a slit moving through a 1–1.5 arcsec wide feature) should be seen as a temporal change in a single small-scale phenomenon. Taking into consideration that the SUMER spatial resolution is ~1.5″, we believe that the radiance and Doppler shift variations detected in the BP correspond to a small-scale phenomenon. Such a phenomenon could be a brightening of a tiny loop forming the BP as already observed by Sheeley & Golub (1979) and suggested by Habbal et al. (1990). However, it could also be due to over-imposed small-scale ejection like features such as spicules. The radiance plot in Fig. 10 better presents the nature of these brightenings. It shows the radiance variations in the bright point at the position marked with a dotted line in Fig. 9. The radiance variations are ~2–3 times above the mean BP radiance. The temporal variations of the Doppler shift corresponding to the same location of the BP is shown in the lower panel of Fig. 10. The 6 min grid helps to distinguish the correlation between the radiance and Doppler shift variations which clearly show that the radiance variations are generally accompanied by a red-shifted emission. The Doppler shift in the BP are in the range from -10 to $+10$ km s^{-1} as the small-scale BP brightenings show velocity variations in the range 3–6 km s^{-1}. A puzzling feature is the appearance of a blue-shifted emission in the center of the BP corresponding to the middle of the scanning period.

There are different possible interpretations of this result. First, it could be an up-flow of the whole bright point (i.e. a phenomenon resembling the rising cold loops sometimes observed during solar flares) with over-exposed brightening events, or this blue-shift which clearly appears in-between the two polarities is the predominant emission of the underlying plasma. A third possibility, is that this emission is due to a possible small-scale reconnection jet. None of these interpretations, however, can be proved in the present study. We expect forthcoming studies to answer this question.

The CDS observations revealed an enhanced emission in two or three pixels within the BP at different wavelengths which do not coincide spatially (Fig. 2). This observational fact supports the finding of Habbal et al. (1990) that the peak radiances in different lines (emitted from the chromosphere to the corona) are not always co-spatial, implying that BPs may consist of a complex of small-scale loops at different temperatures.

3.4. Relation to explosive events and blinkers

The observations in the present study also help in clarifying the question whether UV explosive events (Madjarska & Doyle 2003 and references therein) form the structural unit of the BP

phenomena. Earlier *Skylab* observations (Moses et al. 1994) showed that bright points are not related to the explosive event phenomena. Our study based on continuous and higher resolution observations confirms this fact, at least for the present event. With the exception of one explosive event, which was observed at the border of the BP, we did not register any particular enhanced emission in the blue or/and red wings of the observed line within the BP which may account for an explosive event phenomenon. The appearance of an explosive event at the border of the BP is not a surprising fact because they are typical of the regions at the border of network lanes. Different lines in Fig. 11 correspond to the S VI line profile at the BP (solid line), the network (dashed line) and the explosive event (dotted line). The BP line profile shows no wing enhancements and/or any particular difference with the typical network profile except for the higher counts detected. Moreover, Teriaca et al. (2002) presented strong evidence that explosive events do not reach coronal temperatures and, hence, cannot be the structural unit of the BP phenomena. The appearance of small-scale brightenings with the duration and size similar to those found within blinkers (Chae et al. 2000; Madjarska & Doyle 2003) could suggest a possible relation between blinkers and BPs. Both phenomena are located at the network junctions and were associated with bipolar magnetic regions (Bewsher et al. 2002; Madjarska & Doyle 2003). Unlike most of the blinker phenomena which have only a modest presence in Mg IX, BPs usually show strong emission in this line. If we consider, however, that the mechanism (whatever it is) responsible for the bright point appearance at coronal temperatures (i.e. the heating mechanism) is not always efficient enough to heat the plasma up to coronal temperatures, then we will see the resulting event only in lines emitted at lower temperature.

4. Discussion and conclusions

We have examined the temporal and spatial evolution of a coronal bright point registered simultaneously by four instruments (EIT, MDI, SUMER and CDS) on-board SoHO. For the first time we were able (as far as we are acquainted with the publications) to perform a high resolution spectroscopic analysis using data obtained by the SUMER spectrograph. The evolution of the BP from its formation until its full disappearance in the solar corona has been analysed. The results of this study can be summarized as follows:

At the time when we first detect the BP at coronal temperatures, the two opposite magnetic polarities were at a distance of ~7000 km. Schrijver et al. (1997) concluded in their study
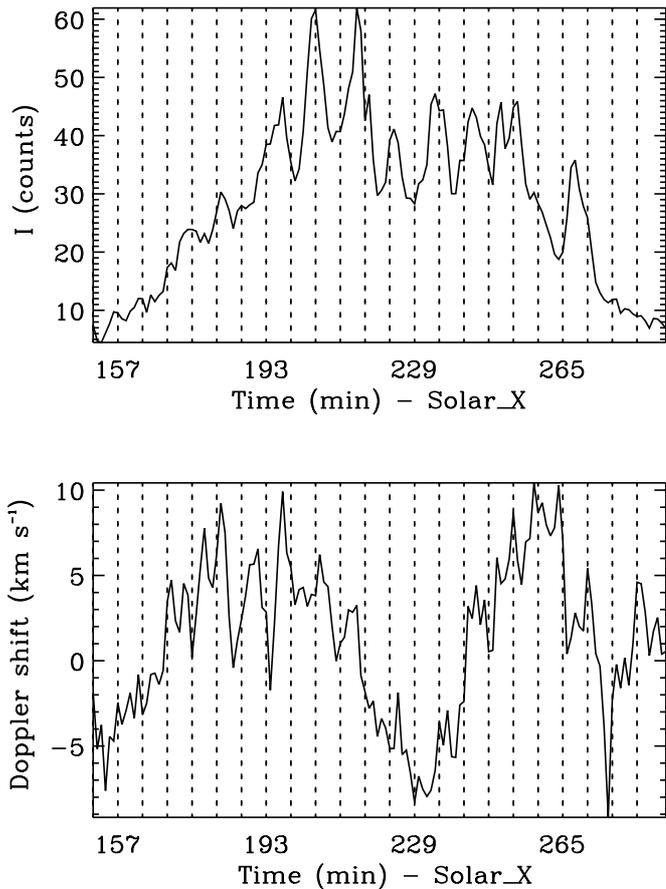
Fig. 10. Line amplitude variations (top panel) and Doppler shift (bottom panel) of the S VI profile for a single pixel in the BP area (the location is shown as a dotted line in Fig. 9). The 6 min grid on these plots helps to identify the correlation between the Doppler shift and line amplitude variations.

Fig. 11. Mean S VI line profile in the BP (solid line), the network (dashed line) and during an UV explosive event (dotted line). The regions which has been used to obtain the line profile in the network and the BP are indicated with a solid and dashed rectangular boxes in Fig. 9, respectively. The location of the explosive event is outside the field of view of Fig. 9 and is marked by a cross in Fig. 1.

of EIT Fe XII 195 Å images and MDI magnetograms that coronal brightenings form between approaching opposite magnetic polarities when the magnetic field concentrations are between 5000 and 25 000 km apart and persist in flux cancellation until the polarities are 2500 to 5000 km apart. They registered only one case where the polarities touched each other. In our case, however, the BP remained during the full period of magnetic field cancellation until the full disappearance of one of the polarities. The decrease of the bipole total unsigned magnetic flux and surface size strongly correlates with the emitting surface and intensity flux decrease in the Fe XII corona. More examples are, however, needed in order to determine whether the full cancellation of one of the polarities or both is a common behaviour of BPs or is only a separate class of coronal BPs.

The spectroscopic analysis is an important contribution to the present work. It revealed that the BP consists of numerous small-scale, short-lived brightenings. The Doppler shift appeared to be of the order of -10 to $+10$ km s^{-1} and no relation to explosive events was found. The appearance of the small-scale brightenings is mostly accompanied by a red-shifted emission. A change-over from red to blue-shift and back to red-shifted emission within 30 min was also observed. We propose that this could be due to an upflow, in the form of
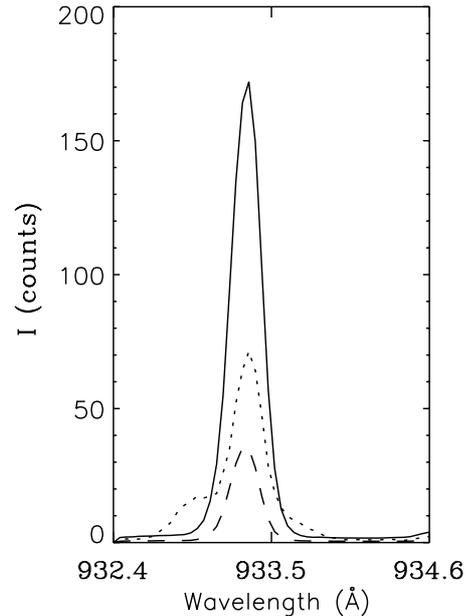
a possible small-scale reconnection jet partially unresolved in our observations, although other hypothesis could be possible.

The next question one can ask is, "Do the brightenings identified in this BP represent the so called "microflares" in XBPs?" Microflares in XBPs were already studied by many authors. Nolte et al. (1979) observed with *Skylab* S–054 impulsive brightenings ($\lesssim$5 min) in two XBPs with 90 s time resolution data. They suggested that these intensity variations are the signature of episodic heating superimposed upon continuous input of energy. Sheeley & Golub (1979) observed that the BPs are made up of small bright loops which turn off and on with a timescale of $\sim$6 min. Habbal et al. (1990) found that brightenings in EUV BPs at different wavelengths with the same duration are not co-spatial. These and other observational facts lead Parker (1988) to conclude that "these occasional brightenings in the emission rise to the level of microflares, so that the XBP seems to be a scaled down version of the large normal active region". Shimojo & Shibata (1999) examined the occurrence rate of microflares (transient brightenings) in a XBP during its lifetime observed with Yohkoh soft X-ray telescope. They found that the occurrence rate (number of events per hour) did not change much during the lifetime of the XBP, although the magnetic flux of the XBP changed. They found an average occurrence rate of 1 microflare every 15 min. These observations, however, are still difficult to link up with our spectroscopic results, but the difference of the brightening occurrence rate could be due to the different spectral, spatial and temporal resolution of the instruments.

Moore et al. (1977) presented another observational fact which showed that X-ray BPs often produce Hα macrospicules. The authors used Hα and X-ray observations of so called

"flares" in X-ray BPs situated on the limb which appeared to be in fact macrospicules. It is difficult to conclude from a spectroscopic study of a single BP the real nature of these transient brightenings. To explore this problem in detail more multi-wavelength and multi-instrument (spectrograph, imager and magnetograph) data are needed. We hope that the present (SoHO and TRACE) and future (Solar-B, SDO and Solar Orbiter) missions will provide us with this opportunity.

References

Bewsher, D., Parnell, C. E., & Harrison, R. A. 2002, Sol. Phys., 206, 21

Chae, J., Haimin, W., & Goode, Ph. 2000, ApJ, 528, 119

Curdt, W., Feldman, U., Laming, J. M., et al. 1997, A&AS, 126, 281

Curdt, W., Brekke, P., Feldman, U., et al. 2001, A&A, 375, 591

Delaboudiniere, J.-P., Artzner, G. E., Brunaud, J., et al. 1995, Sol. Phys., 162, 291

Fisher, G., Langcope, D., Metcalf, T. R., & Pevtsov, A. A. 1998, ApJ, 508, 885

Golub, L., Krieger, A. S., Silk, J. K., Timothy, A. F., & Vaiana, G. S. 1974, ApJ, 189, 193

Golub, L., Krieger, A. S., Harvey, J. W., & Vaiana, G. S. 1977, Sol. Phys., 53, 111

Golub, L. 1980, Phil. Trans. Roy. Soc. London, 297, 595

Habbal, S. R., & Withbroe, G. L. 1981, Sol. Phys., 69, 77

Habbal. S. R., Dowdy, J. F. Jr., & Withbroe, G. L. 1990, ApJ, 352, 333

Habbal, S. R. 1992, Ann. Geophis., 10, 34

Handy, B. N., & Schrijver, C. 2001, ApJ, 547, 1100

Harrison, R. A., Sawyer, E. C., Carter, M. K., et al. 1995, Sol. Phys., 162, 233

Longcope, D. W. 1998, ApJ, 507, 433

Lemaire, P., Wilhelm, K., Curdt, W., et al. 1997, Sol. Phys., 170, 105

Madjarska, M. S., & Doyle, J. G. 2003, A&A, submitted

Moses, D., Cook, J. W., Bartoe, J.-D. F., et al. 1994, ApJ, 430, 913

Nolte, J. T, Solodyna, C. V., & Gerassimenko, M. 1979, Sol. Phys., 63, 113

Parker, E. N. 1988, ApJ, 330, 474

Parnell, C. E., Priest, E. R., & Golub, L. 1994a, Sol. Phys., 151, 57

Parnell, C. E., Priest, E. R., & Titov, V. S. 1994b, Sol. Phys., 153, 217

Preś, P., & Philips, K. J. H. 1999, ApJ, 510, L73

Priest, E. R., Parnell, C. E., & Martin, S. 1994, ApJ, 427, 459

Sheeley, N. R. Jr., & Golub, L. 1979, Sol. Phys., 63, 119

Scherrer, P. H., Bogart, R. S., Bush, R. I., et al. 1995, Sol. Phys., 162, 129

Schrijver, C. J., Shine, R. A., Hurlburt, N. E., Tarbell, T. D., & Lemen, J. R. 1997, Proc. of the Fifth SOHO Workshop, ESA SP-404, 669

Shimojo, M., & Shibata, K. 1999, ApJ, 516, 934

Teriaca, L., Madjarska, M. S., & Doyle, J. G. 2002, A&A, 392, 309

Vaiana, G. S., Krieger, A. S., van Speybroek, L. P., & Zehnpfenning, T. 1970, Bull. Am. Phys. Soc., 15, 611

Webb, D. F. 1986, in Coronal and Prominence Plasmas, NASA CP-2442, ed. A. I. Poland, p. 329

Webb, D. F., Martin, S. F., Moses, D., & Harvey, J. W. 1993, Sol. Phys., 144, 15

Wilhelm, K., Curdt, W., Marsch, E., et al. 1995, Sol. Phys., 162, 189

Wilhelm, K., Lemaire, P., Curdt, W., et al. 1997, Sol. Phys., 170, 75

Zhang, J., Kundu, M. R., & White, S. M. 2001, Sol. Phys., 198, 347